0026-895X/08/7404-952–963$20.00
MOLECULAR PHARMACOLOGY
Copyright © 2008 The American Society for Pharmacology and Experimental Therapeutics
Mol Pharmacol 74:952–963, 2008

Vol. 74, No. 4
49395/3383094
Printed in U.S.A.

Keratinocyte-Derived Vascular Endothelial Growth Factor Biosynthesis Represents a Pleiotropic Side Effect of Peroxisome Proliferator-Activated Receptor-γ Agonist Troglitazone but Not Rosiglitazone and Involves Activation of p38 Mitogen-Activated Protein Kinase: Implications for Diabetes-Impaired Skin Repair[S]

Dana Schiefelbein, Oliver Seitz, Itamar Goren, Jan Philipp Dißmann, Helmut Schmidt, Malte Bachmann, Robert Sader, Gerd Geisslinger, Josef Pfeilschifter, and Stefan Frank

Pharmazentrum Frankfurt/ZAFES (D.S., O.S., I.G., J.P.D., H.S., M.B., G.G., J.P., S.F.) and Zentrum der Chirurgie (R.S.), Klinikum der Johann Wolfgang Goethe-Universität, Frankfurt am Main, Germany

Received June 2, 2008; accepted July 1, 2008

ABSTRACT

The peroxisome proliferator-activated receptors (PPARs) represent pharmacological target molecules to improve insulin resistance in type 2 diabetes mellitus. Here we assessed a functional connection between pharmacological activation of PPAR and vascular endothelial growth factor (VEGF) expression in keratinocytes and during diabetes-impaired acute skin repair in *obese/obese* (*ob/ob*) mice. PPARβ/δ agonist 4-[3-[4-acetyl-3-hydroxy-2-propylphenoxy)propoxy]phenoxy]acetic acid (L165,041) and PPARγ agonists ciglitazone and troglitazone, but not rosiglitazone, potently induced VEGF mRNA and protein expression from cultured keratinocytes. Inhibitor studies revealed a strong functional dependence of troglitazone- and L165,041-induced VEGF expression on p38 and p42/44 mitogen-activated protein kinase (MAPK) activation in keratinocytes. Rosiglitazone also induced activation of p38 MAPK but failed to mediate the activation of p42/44 MAPK in the cells. Functional ablation of PPARβ/δ and PPARγ from keratinocytes by small interfering RNA did not abrogate L165,041- and troglitazone-induced VEGF biosynthesis and suggested VEGF induction as a pleiotropic, PPAR-independent effect of both drugs in the cells. In accordance with the in vitro situation, we found activated p38 MAPK in wound keratinocytes from acute wounds of rosiglitazone- and troglitazone-treated diabetic *obese/obese* mice, whereas keratinocyte-specific VEGF protein signals were only prominent upon troglitazone treatment. In summary, our data from cell culture and wound healing experiments suggested p38 MAPK activation as a side effect of thiazolidinediones; however, only troglitazone, but not rosiglitazone, seemed to translate p38 MAPK activation into a PPARγ-independent induction of VEGF from keratinocytes.

Recent decades have shown a dramatic increase in obesity worldwide. Sedentary lifestyle and consumption of high-caloric food represent the major causes for the obesity "epidemic" in developed countries (Friedman, 2003). This obesity is associated with an increased risk to develop an insulin resistance and type 2 diabetes mellitus. In addition to this concept, there is now strong evidence that immune responses and obesity are tightly connected and that insulin resistance has to be regarded as a functional consequence of adipose tissue-driven inflammatory processes (Hotamisligil, 2006).

Thiazolidinediones (TZDs) represent a class of antidiabetic

This work was supported by the Deutsche Forschungsgemeinschaft (SFB 553, grant FR 1540/1-2, GRK 1172).
D.S. and O.S. contributed equally to this work.
Article, publication date, and citation information can be found at http://molpharm.aspetjournals.org.
doi:10.1124/mol.108.049395.
[S] The online version of this article (available at http://molpharm.aspetjournals.org) contains supplemental material.

ABBREVIATIONS: TZD, thiazolidinedione; PPAR, peroxisome proliferator-activated receptor; VEGF, vascular endothelial growth factor; L165,041, 4-[3-[4-acetyl-3-hydroxy-2-propylphenoxy)propoxy]phenoxy]acetic acid; MAPK, mitogen-activated protein kinase; siRNA, small interfering RNA; TNF, tumor necrosis factor; IL, interleukin; nt, nucleotide; GAPDH, glyceraldehyde-3-phosphate dehydrogenase; EGF, epidermal growth factor; WTM, wortmannin; Act D, actinomycin D; LPS, lipopolysaccharide; IFN-γ, interferon-γ; ELISA, enzyme-linked immunosorbent assay; ANOVA, analysis of variance; PI3K, phosphoinositide 3-kinase; wm, wound margin; iw, inner wound; WY14643, 4-chloro-6-(2,3-xylidino)-2-pyrimidinyl-)thioacetic acid; U0126, 1,4-diamino-2,3-dicyano-1,4-bis(methylthio)butadiene; SB203580, 4-(4-fluorophenyl)-2-(4-methylsulfinylphenyl)-5-(4-pyridyl)1*H*-imidazole; GW9662, 2-chloro-5-nitrobenzanilide.

drugs that are capable of improving insulin resistance in target tissues such as muscle and liver (Henry, 1997). In 1995, it became clear that TZDs act through activation of the nuclear hormone receptor peroxisome proliferator-activated receptor (PPAR)-γ (Lehmann et al., 1995). The PPAR family of transcription factors consists of two additional members: PPARα and PPARβ/δ, and all members heterodimerize with 9-*cis*-retinoic acid retinoid X receptors (Kliewer et al., 1992, 1994). Insulin resistance now seems to be a consequence of the release of cytokines and adipokines from growing adipose tissue under conditions of obesity (Hotamisligil, 2006; Tilg and Moschen, 2006). TZDs interfere with the endocrine signaling process of adipocytes to muscle and liver and enhance insulin action in these organs through down-regulation of tumor necrosis factor (TNF)-α and IL-6 and induction of the insulin-sensitizing hormone adiponectin in adipose tissue (Rangwala and Lazar, 2004). It is interesting that hyperlipidemia, representing an additional obesity-associated risk factor, can be improved by fibrates that activate PPARα (Staels and Fruchart, 2005).

Diabetes-associated severe ulcerations of the skin represent a serious problem of growing clinical importance. Diabetic ulcers still have a poor prognosis with high reulceration rates and a high mortality after limb amputations (Faglia et al., 2001). Besides their metabolic functions, it is interesting that PPARα, -β/δ, and -γ have been shown also to be involved in the homeostatic regulation of normal and injured skin (Michalik and Wahli, 2007). Epidermal keratinocytes express all three PPAR isoforms (Rivier et al., 1998). In these cells, PPARβ/δ is the major isoform, whereas PPARα and PPARγ are increased and functionally connected to keratinocyte differentiation in humans and mice (Rivier et al., 1998; Kömüves et al., 2000; Mao-Qiang et al., 2004). In contrast to PPARγ, which remains hardly detectable upon skin wounding, PPARα and -β/δ are reactivated in wound margin keratinocytes during acute healing in mice (Michalik et al., 2001). Keratinocytes represent a major source of vascular endothelial growth factor (VEGF) in skin wounds (Brown et al., 1992), and VEGF expression is induced by cytokines and growth factors in the cells (Frank et al., 1995). In this study, we investigated the potency of PPAR agonists to interfere with keratinocyte-derived VEGF expression. The PPARγ agonist troglitazone, but not rosiglitazone, potently induced keratinocyte VEGF expression; however, our data constitute evidence that troglitazone-mediated induction of VEGF expression was independent from PPARγ but functionally connected to p38 MAPK activation in cultured keratinocytes.

Materials and Methods

Animals. Female C57BL/6J-*ob*/*ob* mice were obtained from Charles River WIGA (Sulzfeld, Germany) and were maintained under a 12-h light/dark cycle at 22°C until they were 10 weeks of age. At this time, they were caged individually, monitored for body weight, and wounded as described below.

Treatment of Mice. Mice were treated with rosiglitazone (Avandia, 5 mg/kg/day) or troglitazone (5 mg/kg/day) twice a day (6:00 AM and 6:00 PM) by gastrogavage for the indicated time points. The drug was freshly homogenized in 0.5% methylcellulose (Fluka; Sigma-Aldrich, Seelze, Germany) before oral administration. Treatment of mice with 0.5% methylcelluose alone served as a control. Rosiglitazone (Avandia) was from GlaxoSmithKline Consumer Healthcare (Bühl, Germany), and troglitazone was from Axxora (Lörrach, Germany).

Wounding of Mice. Wounding of mice was performed as described previously (Frank et al., 1999; Stallmeyer et al., 1999). In brief, mice were anesthetized with a single intraperitoneal injection of ketamine (80 mg/kg body weight)/xylazine (10 mg/kg body weight). Six full-thickness wounds (5 mm in diameter, 3–4 mm apart) were made on the back of each mouse by excising the skin and the underlying panniculus carnosus. An area measuring 7 to 8 mm in diameter, which included the granulation tissue and the complete epithelial margins, was excised at the indicated time points for analysis. As a control, a similar amount of skin was taken from the backs of nonwounded mice. For each experimental time point, tissue from four wounds each from three animals (n = 12 wounds, RNA analysis) and from two wounds each from three animals (n = 6 wounds, protein analysis) were combined and used for RNA and protein preparation. All animal experiments were carried out according to the guidelines and were approved by the local ethics animal review board.

RNA Isolation and RNase Protection Analysis. RNA isolation and RNase protection assays were carried out as described previously (Chomczynski and Sacchi, 1987; Frank et al., 1999). The cDNA probes were cloned using reverse transcription-polymerase chain reaction. The murine probes corresponded to nt 139 to 585 (VEGF, S38083), nt 1499 to 1779 (for PPARβ/δ, NM_006238), and nt 163 to 317 (for GAPDH, NM_002046). The human probes corresponded to nt 1362 to 1516 (for VEGF, NM_001025370.1) and nt 961 to 1070 (for GAPDH, M33197), respectively.

Immunohistochemistry. Mice were wounded as described above. Animals were sacrificed at day 5 after injury. Complete wounds were isolated from the back and fixed in formalin. Bisected wounds were embedded in paraffin. Immunohistochemistry from 4-μm deparaffinized serial sections was performed as described previously (Stallmeyer et al., 1999). Sections were stained with the avidin-biotin-peroxidase complex system using 3,3-diaminobenzidine-tetrahydrochloride as a chromogenic substrate. Nuclei were counterstained with hematoxylin. The antibody directed against murine VEGF was from Santa Cruz (Heidelberg, Germany). The phosphospecific anti-p38 MAPK antibody was obtained from Cell Signaling Technology (Frankfurt, Germany).

Cell Culture. Human HaCaT epidermal keratinocytes (Boukamp et al., 1988) were grown to confluence in Dulbecco's modified Eagles's medium (Invitrogen AG, Karlsruhe, Germany). Human primary keratinocytes were isolated according to a protocol from PromoCell (available at http://www.promocell-academy.com) and cultured in keratinocyte growth medium 2 (PromoCell, Heidelberg, Germany). The murine macrophage cell line RAW264.7 was cultured in RPMI medium (Invitrogen AG). Confluent keratinocytes were subsequently treated with epidermal growth factor (EGF; 10 ng/ml), ciglitazone (0.1–25 μM), troglitazone (0.1–25 μM), rosiglitazone (0.1–50 μM), L165,041 (0.1–50 μM), WY14643 (50 μM), clofibrate (500 μM) in the presence or absence of 200 nM wortmannin (WTM), 10 μM U0126, 5 μM SB203580, or 10 μM actinomycin D (Act D) for the indicated periods of time. RAW264.7 cells were stimulated with lipopolysaccharide (LPS; 200 ng/ml) and interferon-γ (IFN-γ; 2 ng/ml). EGF and IFN-γ were purchased from Roche Biochemicals (Mannheim, Germany). WTM and SB203580 were obtained from Calbiochem (Darmstadt, Germany), and U0126 was from Alexis (San Diego, CA). Ciglitazone, troglitazone, L165,041, WY14643, and clofibrate were obtained from Merck (Darmstadt, Germany). Rosiglitazone was from Axxora (Lörrach, Germany). LPS was from Sigma (Taufkirchen, Germany).

Nitrite Determination in Cell Culture Supernatants. Nitrite, a stable nitric oxide (NO) oxidation product, was determined in cell culture supernatants using the Griess reaction (Green et al., 1982). In brief, cleared supernatants were mixed with 20 μl of sulfanilamide (dissolved in 1.2 M HCl) and 20 μl of *N*-naphthylethyl-

enediamine dihydrochloride. After 5 min, the absorbance was measured at 540 nm.

Determination of Cell Viability. Viability of cultured keratinocytes was assessed using the 3-(4,5-dimethylthiazol-2-yl)-2,5-diphenyltetrazolium assay by following a published protocol (Mosmann, 1983).

Enzyme-Linked Immunosorbent Assay. Quantification of human $VEGF_{165}$ protein from keratinocyte cell culture supernatants was performed using the human VEGF enzyme-linked immunosorbent assay (ELISA) kit (Biosource, Nivelles, Belgium).

Preparation of Protein Lysates and Immunoblot Analysis. Keratinocyte cell culture samples and murine skin were homogenized as described previously (Goren et al., 2006). Twenty to fifty micrograms of total protein lysate was separated using SDS-gel electrophoresis, and specific proteins were detected using antisera directed against total Akt, phospho-Akt (Ser473), phospho-p38 MAPK (Thr180, Tyr182), phospho-p42/44 MAPK (Thr202, Tyr204) (Cell Signaling, New England Biolabs), PPARγ (Santa Cruz), and β-actin (Sigma). A secondary antibody coupled to horseradish peroxidase and the enhanced chemiluminescence detection system was used to visualize the proteins of interest. Phenylmethylsulfonyl fluoride, aprotinin, NaF, Na_2VO_4, and dithiothreitol were from Sigma. Ocadaic acid and leupeptin were from BioTrend (Köln, Germany), and the enhanced chemiluminescence detection system was obtained from GE Healthcare (Freiburg, Germany).

Silencing of PPARγ and PPARβ/δ Expression by Small Interfering RNA. HaCaT keratinocytes (2×10^5) were grown in six-well plates to reach 40 to 60% confluence. Cells were subsequently transfected twice with the respective small interfering RNA (siRNA; 50 nM final concentration) using Oligofectamine (Invitrogen, Karlsruhe, Germany) and Opti-MEM (Invitrogen) as described by the manufacturer.

Determination of Rosiglitazone and Troglitazone in Mouse Plasma Samples by Liquid Chromatography/Mass Spectrometry/Mass Spectrometry. Aliquots of mouse plasma samples were extracted by methanol/water (50:50 v/v) precipitation. Pioglitazone and ciglitazone were used as internal standards for rosiglitazone and troglitazone, respectively. HPLC analysis was done under gradient conditions using a Luna C18(2) column (Phenomenex, Aschaffenburg, Germany). Mass spectrometry and tandem mass spectrometry analyses were performed on a 4000 Q TRAP triple-quadrupole mass spectrometer with a Turbo V source (Applied Biosystems, Darmstadt, Germany) in the negative ion mode. Precursor-to-product ion transitions of m/z 356→42 for rosiglitazone, 440→42 for troglitazone, 355→42 for pioglitazone, and m/z 332→42 for ciglitazone were used for the multiple reaction monitoring with a dwell time of 150 ms. Concentrations of the calibration standards, quality controls, and unknowns were evaluated by Analyst software (version 1.4; Applied Biosystems). Variations in accuracy and intraday and interday precision ($n = 6$ for each concentration, respectively) were <15% over the range of calibration.

Statistical Analysis. Data are shown as means ± S.D. Data analysis was carried out using the unpaired Student's t test with raw data. Statistical comparison between more than two groups was carried out by analysis of variance (ANOVA; Dunnett's method).

Results

Troglitazone and L165,041 but Not Rosiglitazone Potently Induce VEGF Expression in Keratinocytes. Epidermal keratinocytes express all three PPAR subtypes (Rivier et al., 1998). Because angiogenesis is central to skin repair (Singer and Clark, 1999; Eming and Krieg, 2006) and

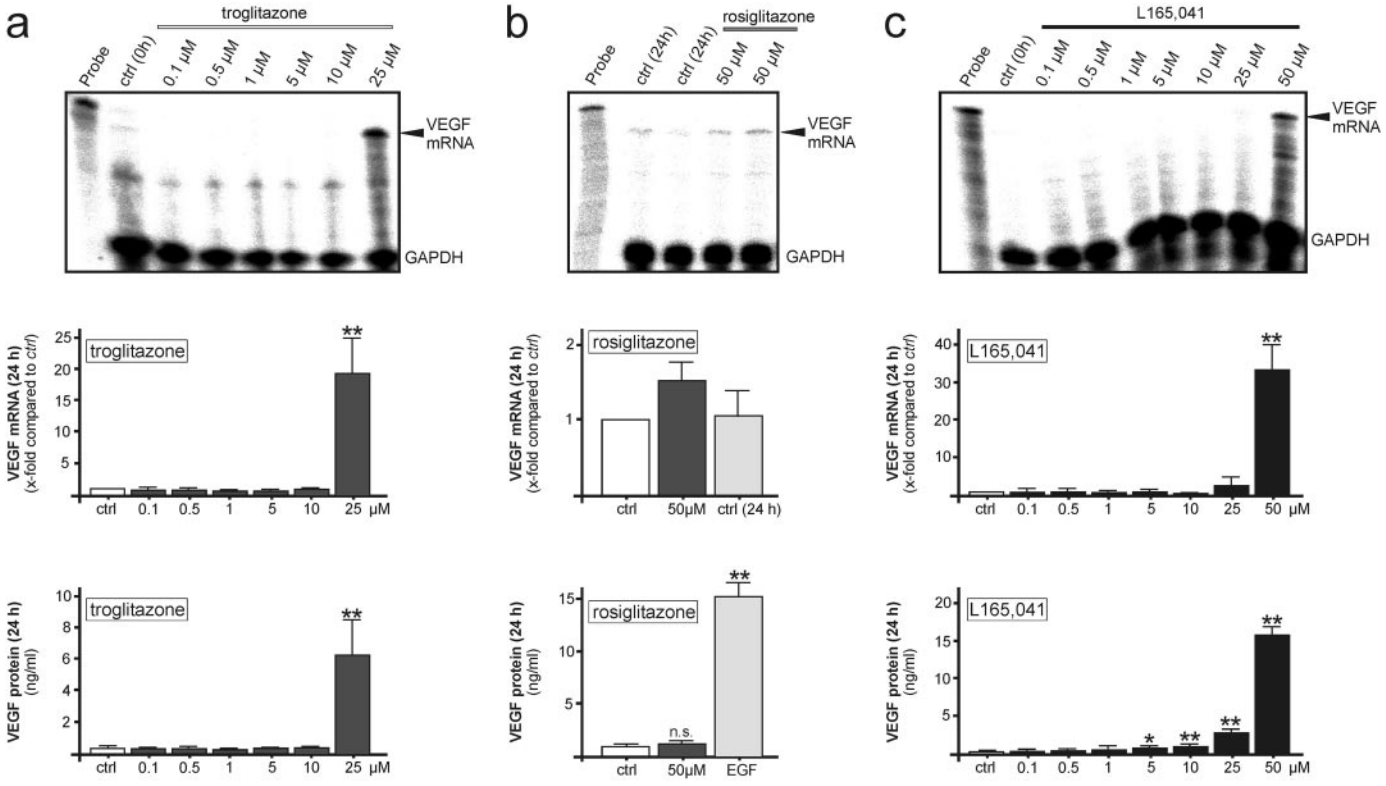

Fig. 1. Dose-dependent induction of VEGF expression in keratinocytes by PPAR agonists. Quiescent human HaCaT keratinocytes were stimulated with troglitazone (a), rosiglitazone (b), or L165,041 (c) for 24 h as indicated. EGF (10 ng/ml) was used as a control. After 24 h, VEGF mRNA expression of nonstimulated (ctrl) or stimulated keratinocytes was analyzed by RNase protection assay (top and middle). $VEGF_{165}$ protein release from the cells was assessed by ELISA analyses of the corresponding conditioned cell culture supernatants (bottom). **, $P < 0.01$; *, $P < 0.05$; n.s., not significant compared with nonstimulated control cells (ctrl). Bars indicate the mean ± S.D. from three independent cell culture experiments ($n = 3$).

keratinocytes are well known producers of VEGF at the wound site (Brown et al., 1992) and in vitro (Frank et al., 1995), we tested the potency of diverse PPAR agonists to drive VEGF expression in keratinocytes. The PPARγ agonists troglitazone (Fig. 1a), ciglitazone (Supplemental Figure S1), and the PPARβ/δ agonist L165,041 (Fig. 1c) are potent inducers of VEGF mRNA (top and middle) and protein (bottom) expression in cultured human HaCaT keratinocytes. By contrast, the PPARγ agonist rosiglitazone failed to induce VEGF expression in the cells at low (0.1–25 μM; data not shown) and even at highest concentrations (Fig. 1b). It is interesting that the dose-response experiment revealed that the PPARγ agonists troglitazone and ciglitazone or the β/δ agonist L165,041 mediated an "on/off" phenomenon with respect to VEGF expression at higher concentrations (glitazones, 25 μM; L165,041, 50 μM) (Fig. 1, a and c; Supplemental Figure S1). By contrast, PPARα agonists WY14643 (50 μM) and clofibrate (500 μM) did not induce VEGF mRNA and protein expression in keratinocytes even at the highest concentrations (data not shown).

As a next step, we determined the kinetics of VEGF expression in keratinocytes using the effective concentration of respective PPARγ (troglitazone and ciglitazone only, because rosiglitazone did not induce VEGF) and β/δ agonists. PPARγ agonists troglitazone (Fig. 2a) and ciglitazone (Supplemental Figure S2) or the PPARβ/δ agonist L165,041 (Fig. 2b) mediated a steady increase in VEGF mRNA (top) and protein (bottom) expression in keratinocytes. In contrast to rosiglitazone (Fig. 1b), the PPAR agonists troglitazone and L165,041 induced a dramatic stimulation of VEGF mRNA (20- to 60-fold) and the release of large amounts of VEGF protein (5–20 ng/ml) into the cell culture supernatants.

To test the bioactivity of rosiglitazone, we assessed the ability of this drug to suppress the proinflammatory stimulation of murine macrophages in vitro. LPS and IFN-γ, which characteristically trigger macrophage inflammatory activity (Gordon, 2003), potently mediated the accumulation of nitrite in cell culture supernatants of stimulated RAW264.7 macrophages. Nitrite represents a reliable readout for inducible nitric-oxide synthase activity. Rosiglitazone (50 μM) turned out to be effective, because the drug significantly reduced the production of nitrite from activated RAW264.7 macrophages (Fig. 3).

In addition, Fig. 4 demonstrates that human primary keratinocytes responded to troglitazone and L165,041 treatment by increased VEGF mRNA (a) and protein (b) expression. EGF, which is described as a potent inducer of VEGF expression from human keratinocytes (Frank et al., 1995), has been used as positive control in our experimental setting.

Troglitazone and L165,041 Induce VEGF Gene Transcription. To investigate whether the increase in VEGF mRNA was due to an interference of the respective drug with

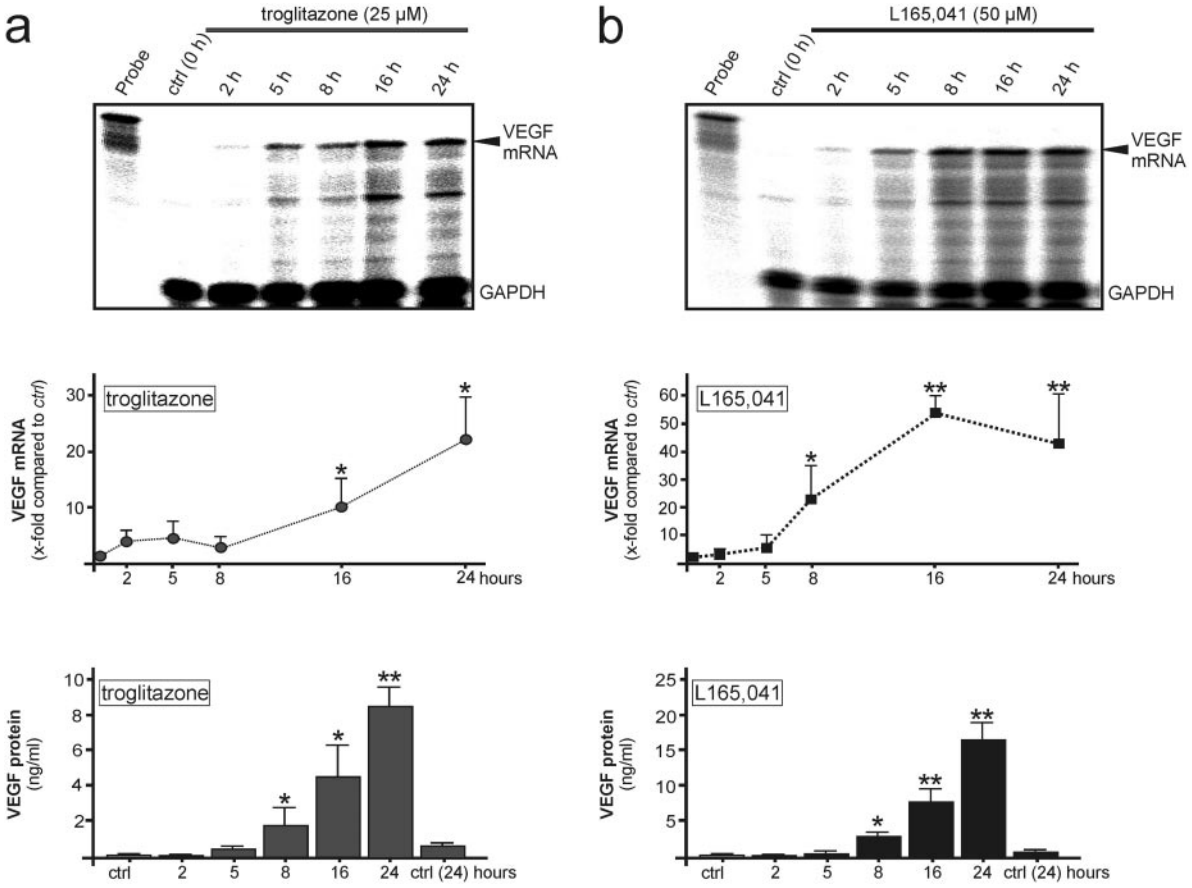

Fig. 2. Time-dependent induction of VEGF expression in keratinocytes by PPAR agonists. Confluent human HaCaT keratinocytes were stimulated with 25 μM troglitazone (a) or 50 μM L165,041 (b) for the indicated time points. At the indicated time points of stimulation, VEGF mRNA expression of nonstimulated (ctrl, 0 h) or stimulated keratinocytes was analyzed by RNase protection assay (top and middle). $VEGF_{165}$ protein release from the cells was assessed by ELISA analyses of the corresponding conditioned cell culture supernatants (bottom). **, $P < 0.01$; *, $P < 0.05$ compared with nonstimulated control cells (ctrl). Bars indicate the mean ± S.D. from three independent cell culture experiments ($n = 3$).

transcriptional or post-transcriptional control mechanisms, we stimulated Act D (10 μM) pretreated keratinocytes with troglitazone or L165,041. In this experimental setting, we did not observe any increase in VEGF mRNA upon stimulation (data not shown). However, troglitazone or L165,041 might contribute to VEGF production by stabilizing the transcriptionally induced VEGF mRNA species. To test this hypothesis, we stimulated the cells with the respective drug for 16 h to induce VEGF mRNA and subsequently added Act D to shut off active transcription. EGF stimulation was performed as control (Frank et al., 1995). As shown in Fig. 5 (top), we observed a rapid decrease of induced VEGF mRNA after Act D-mediated inhibition of transcriptional activity. Independent from the individual potency of the respective drug to induce VEGF expression, we observed a comparable half-life of VEGF mRNA of approximately 4 h for troglitazone, L165,041, or EGF, respectively. Figure 5 (bottom) shows the respective time controls (16 and 24 h) for drugs and EGF, which clearly show that VEGF mRNA was not reduced in the absence of Act D.

Troglitazone- and L165,041-Induced VEGF Expression Is Independent from PPAR Activation. As given in Fig. 6, inhibitor experiments strongly argue for MAPK activation as the functional basis of troglitazone-mediated VEGF expression in keratinocytes. It is noteworthy that inhibition of either p42/44 (by U0126) or p38 (by SB203580) MAPK nearly completely abrogated troglitazone-induced the expression of VEGF mRNA in keratinocytes, whereas inhibition of PI3K by wortmannin had no effect (Fig. 6a, top). As a conse-

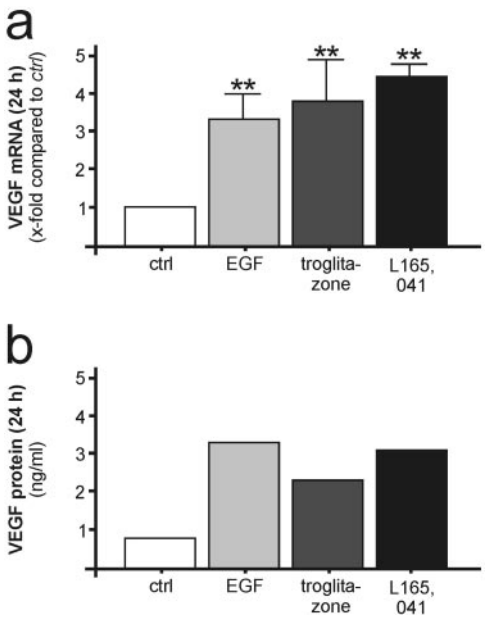

Fig. 4. Induction of VEGF expression by PPARβ/δ and PPARγ agonists in human primary keratinocytes. Quiescent human primary keratinocytes were stimulated with EGF (10 ng/ml), troglitazone (25 μM), or L165,041 (50 μM) for 24 h. After 24 h, VEGF mRNA expression of nonstimulated (ctrl) or stimulated primary keratinocytes was analyzed by RNase protection assay (a). **, $P < 0.01$ compared with nonstimulated control cells (ctrl). Bars indicate the mean ± S.D. from three independent cell culture experiments ($n = 3$). $VEGF_{165}$ protein release from the cells was assessed by ELISA analyses of conditioned cell culture supernatants (b). $VEGF_{165}$ protein expression from one representative experiment is shown.

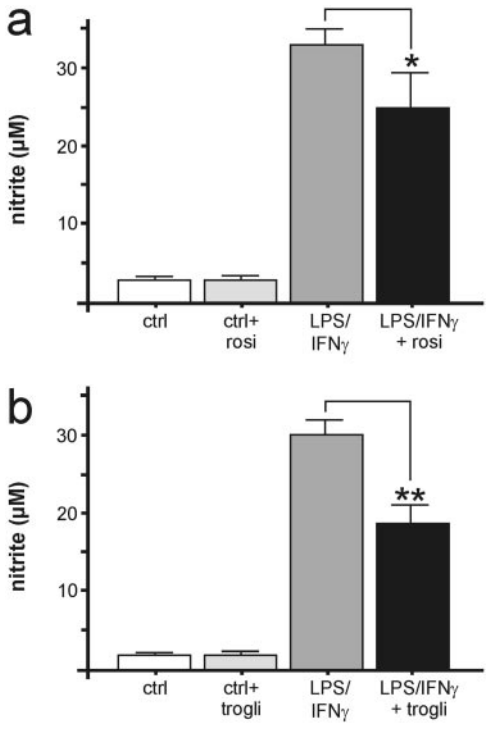

Fig. 3. Rosiglitazone and troglitazone are functionally active. Quiescent murine RAW264.7 macrophages were activated using LPS (200 ng/ml) and IFNγ (2 ng/ml) for 24 h in the presence or absence of 50 μM rosiglitazone (a) or 25 μM troglitazone (b). Nitrite accumulation as an assessment of inducible NOS activity and thus macrophage activation was assessed using the Griess reaction. **, $P < 0.01$; *, $P < 0.05$ as indicated by the bracket. Bars indicate the mean ± S.D. from three independent cell culture experiments ($n = 3$).

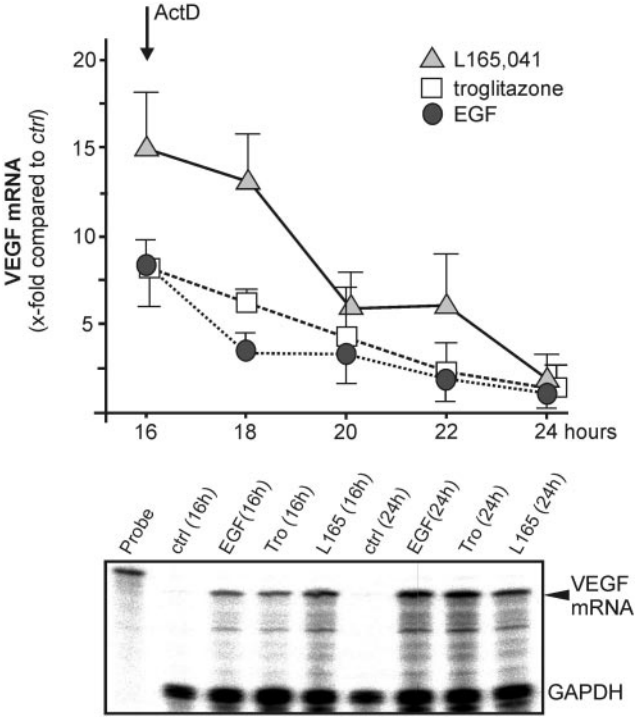

Fig. 5. PPARβ/δ and PPARγ agonists do not stabilize VEGF mRNA. Quiescent HaCaT keratinocytes were stimulated with EGF (10 ng/ml), troglitazone (25 μM), or L165,041 (50 μM) for 16 h. After 16 h, Act D (10 μM) was added to the cells. Keratinocyte VEGF mRNA levels were determined at the indicated time points of treatment by RNase protection assay. Bars indicate the mean ± S.D. from three independent cell culture experiments ($n = 3$). A RNase protection assay demonstrating VEGF mRNA in stimulated keratinocytes in the absence of Act D (16 and 24 h as indicated) is shown at the bottom.

quence, we observed a marked reduction of troglitazone-induced VEGF protein upon inhibition of p42/44 and p38 MAPK at the early 16-h experimental time point, and inhibition of VEGF protein expression remained significantly reduced even after 24 h of stimulation (Fig. 6a, bottom). In addition, induction effects of the PPARβ/δ agonist L165,041 on keratinocyte VEGF mRNA (Fig. 6b, top) and protein (Fig. 6b, bottom) expression seemed to be sensitive to inhibition of PI3K or p42/44 and p38 MAPK activation.

In accordance with wortmannin-insensitive VEGF induction by troglitazone, we observed no increase in phosphorylation of protein kinase B/Akt, which represents a target of active PI3K (Franke et al., 1995) (data not shown). In contrast, troglitazone mediated a strong phosphorylation and thus activation of both p38 and p42/44 MAPK (Fig. 7a). The PPARγ agonist rosiglitazone did not induce VEGF expression in keratinocytes (Fig. 1b); however, the drug shared its capability to potently induce p38 MAPK activation with troglitazone. Rosiglitazone failed to mediate p42/44 MAPK activation (Fig. 7a). Activation of the MAPKs by the assessed drugs in keratinocytes seemed to be independent from a cellular response toward stress or toxicity, because a cell viability assay showed only moderate changes in cell survival upon drug exposure (Fig. 7b).

To unequivocally prove a PPAR-independent mode of action for troglitazone- and L165,041-induced VEGF expression in keratinocytes, we used an siRNA approach to specifically knockdown PPAR expression in the cells. As shown in Fig. 8a, PPARγ-specific siRNA was able to abrogate the observed constitutive expression of PPARγ protein. For unknown reasons, we consistently observed an increase of PPARγ expression in keratinocytes transfected with the scrambled control RNA. Troglitazone mediated a robust induction of keratinocyte VEGF expression in the absence of functional PPARγ (Fig. 8a), clearly demonstrating that specific binding of troglitazone to PPARγ must not be involved in its capability of stimulating VEGF expression in keratinocytes. In accordance, the siRNA-specific knockdown of PPARβ/δ in the cells did not interfere with L165,041-induced VEGF expression, again suggesting a receptor-independent mechanism for L165,041 (Fig. 8b). Please note that we were forced to control the PPARβ/δ knockdown at the mRNA level, because we failed to show convincingly a

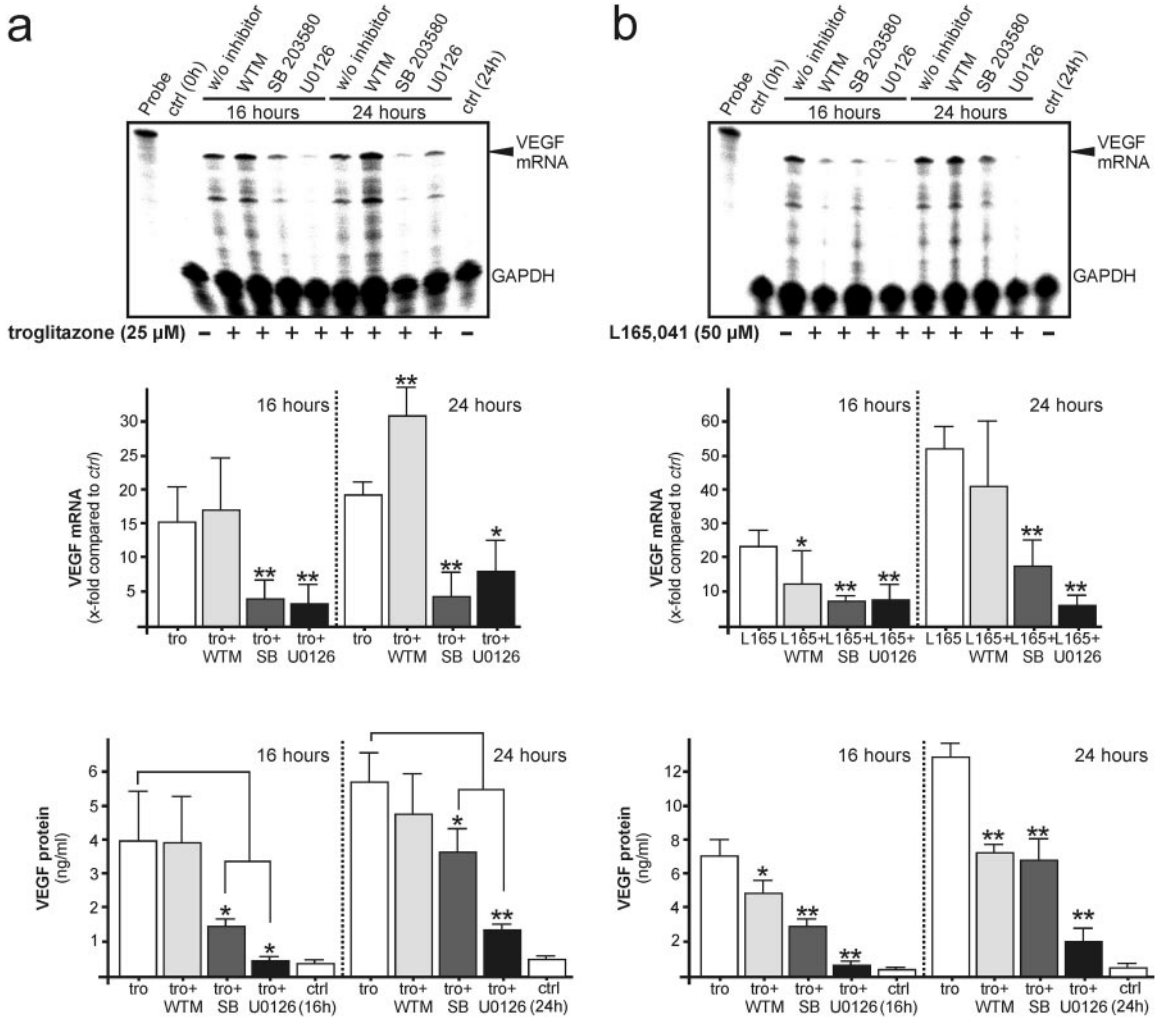

Fig. 6. Troglitazone- and L165,041-mediated VEGF expression is dependent on MAPK activation. Quiescent human HaCaT keratinocytes were stimulated with troglitazone (a) or L165,041 (b) for 16 and 24 h in the absence or presence of WTM (200 nM), SB203580 (5 μM), or U0126 (10 μM) as indicated and subsequently analyzed for VEGF mRNA expression by RNase protection assay (top and middle). $VEGF_{165}$ protein release from the cells was assessed by ELISA analyses of the corresponding conditioned cell culture supernatants (bottom). **, $P < 0.01$; *, $P < 0.05$ compared with stimulated keratinocytes in the absence of the respective inhibitor. Bars indicate the mean ± S.D. from three independent cell culture experiments ($n = 3$).

PPARβ/δ protein expression with different commercially available antibodies (data not shown).

Opposite Effects of PPARγ Agonists Rosiglitazone and Troglitazone on Wound Keratinocytes in Diabetes-Impaired Skin Wounds. PPARγ is only hardly detectable in acute wound tissue and seems to be of minor importance for tissue repair (Michalik et al., 2001). However, because we had demonstrated the robust VEGF induction to be independent from PPARγ in keratinocytes (Figs. 6 and 8), it was interesting to assess a potential therapeutic action of PPARγ agonists to improve the strongly impaired angiogenic process in diabetic wound tissue (Frank et al., 1995; Kämpfer et al., 2001; Stallmeyer et al., 2001; Eming and Krieg, 2006) by stimulating VEGF release from wound keratinocytes. Figure 9 demonstrates the marked loss of VEGF protein expression in acute wound tissue of diabetic *ob/ob* mice. To improve these disturbed conditions, we treated wounded diabetic *ob/ob* mice orally with the PPARγ agonists rosiglitazone or troglitazone, respectively. Liquid chromatography/mass spectrometry/mass spectrometry analysis of blood serum from treated animals revealed the high bioavailability of both drugs: oral administration of 5 mg/kg/day rosiglitazone resulted in

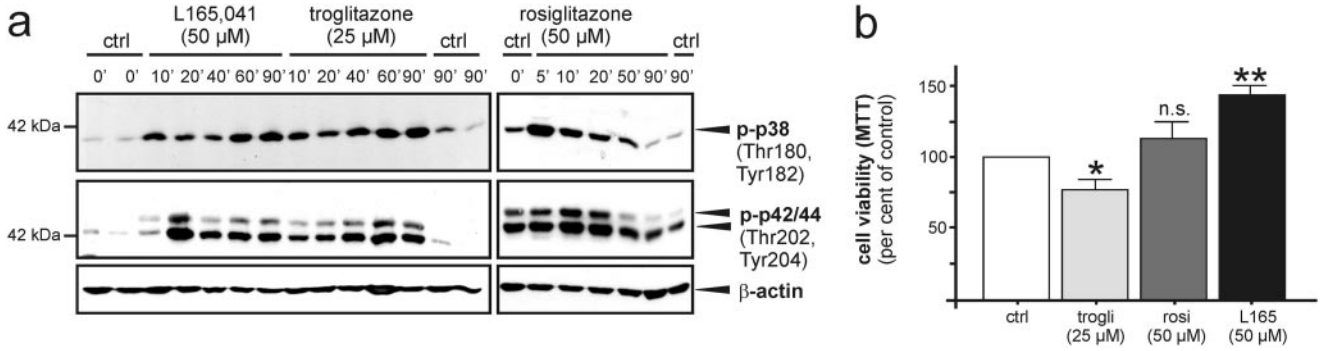

Fig. 7. Differential activation of p38 and p42/44 MAPK by PPAR agonists. a, quiescent HaCaT keratinocytes were treated with L165,041 (50 μM), troglitazone (25 μM), or rosiglitazone (50 μM) for the indicated time periods. Nonstimulated cells (ctrl 0′, ctrl 90′) served as controls. Total cell lysates were analyzed for the presence phosphorylated p38 MAPK (*p-p38 Thr180, Tyr182*) or phosphorylated p42/44 MAPK (*p-p42/44 Thr202, Tyr204*) by immunoblot. Loading of gels was controlled by the analysis of β-actin expression as indicated. b, keratinocyte viability as assessed by 3-(4,5-dimethylthiazol-2-yl)-2,5-diphenyltetrazolium assay in the presence or absence of troglitazone (25 μM), rosiglitazone (50 μM), or L165,041 (50 μM) as indicated. **, $P < 0.01$; *, $P < 0.05$; n.s., not significant compared with nonstimulated control cells (ctrl). Bars indicate the mean ± S.D. from three independent cell culture experiments ($n = 3$).

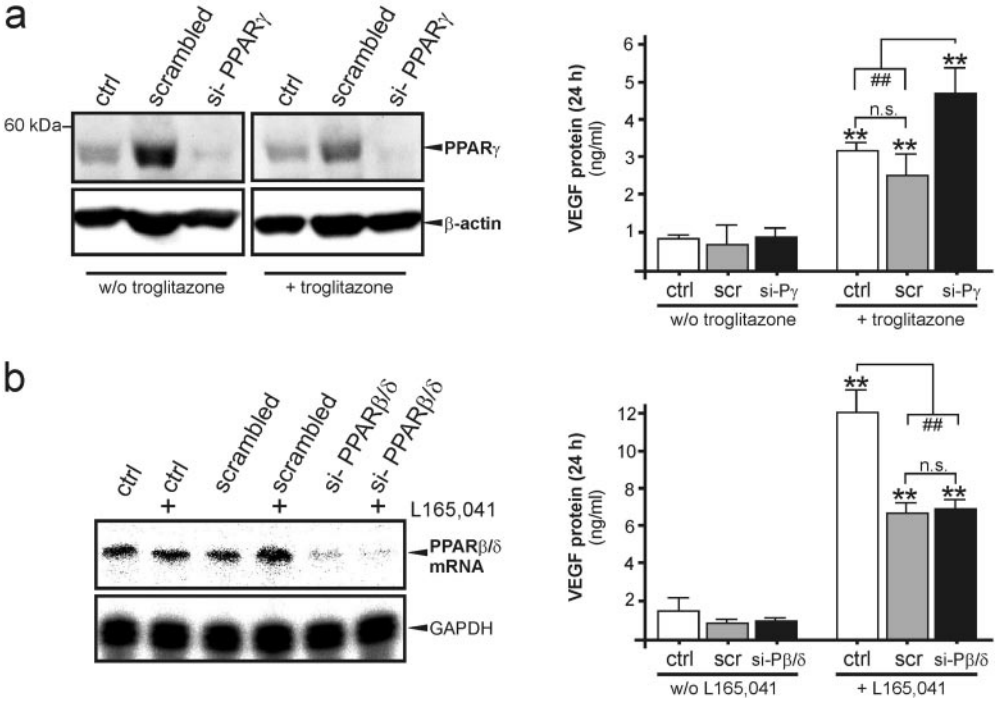

Fig. 8. Troglitazone- and L165,041-induced VEGF expression are independent of PPAR expression. Cultured HaCaT keratinocytes were treated with Oligofectamine alone (ctrl) and in combination with a nonspecific (scrambled) siRNA, a PPARγ-specific siRNA (si-PPARγ) (a) or a PPARβ/δ-specific siRNA (si-PPARβ/δ) (b) as indicated. Abrogation of the respective PPAR in keratinocytes was controlled by immunoblot (a, left) or RNase protection assay (b, left) as indicated. Analysis of β-actin (a) or GAPDH (b) was used to control an equal loading. $VEGF_{165}$ protein release from control- (ctrl), scrambled RNA (scr)- or PPAR-specific siRNA (si-Pγ; si-Pβ/δ)-treated keratinocytes in the absence (w/o) or presence (±) of troglitazone (25 μM) or L165,041 (50 μM) as indicated. **, $P < 0.01$ compared with conditions without drug. ##, $P < 0.01$; n.s., not significant as indicated by brackets. Bars indicate the mean ± S.D. from three independent cell culture experiments ($n = 3$).

average blood serum levels of 12.5 ± 2.5 μg rosiglitazone; oral administration of 5 mg/kg/day troglitazone led to average blood serum levels of 0.9 ± 0.3 μg/ml troglitazone. /ml

Upon treatment of animals, we determined the expression levels of VEGF mRNA from complete acute wound tissue isolated from mock- and rosiglitazone-treated *ob/ob* mice. Only wound tissue from mock-treated animals was characterized by significantly increased VEGF mRNA levels compared with nonwounded skin (Fig. 10a). Although significant in the ANOVA statistical analysis, the difference between mock- and rosiglitazone-administered mice seemed only very moderate in early wounds (Fig. 10a, 1d wound tissue). However, the differences in VEGF mRNA levels upon rosiglitazone treatment turned out to become more pronounced during ongoing repair (Fig. 10a, 5d wound tissue). As a next step, we separated total wound tissue into the wound margin (wm; enriched for wound margin keratinocytes as potential producers of VEGF) and inner wound (iw; contains the granulation tissue) compartments before RNA isolation. Strengthening our data from total wound tissue, we found a marked reduction of VEGF mRNA levels restrictively only at the wm in rosiglitazone-treated *ob/ob* mice (Fig. 10b). Immunohistochemistry data on wound tissue from *ob/ob* mice revealed a detailed insight into the interference of rosiglitazone with tissue repair. In line with mRNA data from wm tissue (Fig. 10b), we observed marked signals of immunoreactive VEGF protein in wound margin keratinocytes of mock-treated *ob/ob* mice (Figs. 10c and 12, top). Rosiglitazone seemed to interfere with VEGF synthesis in impaired wound tissue in two ways: first, by reducing the expression of total VEGF protein in wound keratinocytes (VEGF-specific signals were reduced); and second, by inhibiting overall keratinocyte proliferation, because wound margin epithelia of rosiglitazone-administered mice exhibited an atrophied morphology (Figs. 10c and 12, top). This was in contrast to the effects mediated by troglitazone treatment of mice. Reflecting the in vitro potency to induce VEGF expression in keratinocytes (Figs. 1 and 2), troglitazone mediated a robust VEGF expression in wound margin epithelia (Fig. 12, top). Here, it is noteworthy that VEGF-specific signals in wound keratinocytes from troglitazone-treated *ob/ob* mice seemed even elevated compared with mock-treated animals. Moreover, sizes of wound margin epithelia were also not reduced by troglitazone treatment (Fig. 12, top).

Immunoblots using wound lysates revealed obvious differences in the activation of MAPKs at the wound site upon different drug regimen. Whereas levels of activated p38 were reduced in the presence of unaltered p42/44 phosphorylation in wounds of rosiglitazone- versus mock-treated mice, we found an induction of p42/44 activation and no difference in p38 activation in wound tissue of troglitazone-treated animals (Fig. 11). However, these immunoblots from wound lysates reflected all cell types at the wound site. This is a major disadvantage with respect to our experiments, which

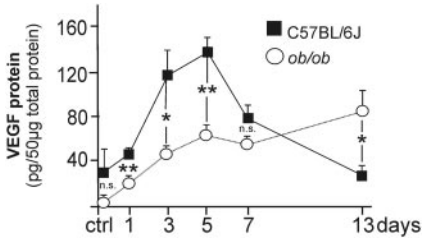

Fig. 9. Impaired VEGF protein expression in acute wounds of diabetic mice. VEGF ELISA analyses from lysates of nonwounded skin (ctrl) and lysates of wound tissue isolated from wild-type (C57BL/6J) and diabetic *ob/ob* mice. VEGF protein is expressed as picograms per 50 μg of skin or wound lysate. **, $P < 0.01$; *, $P < 0.05$; n.s., not significant (unpaired Student's *t* test). Bars indicate the mean ± S.D. obtained from wound lysates from 12 individual mice ($n = 12$).

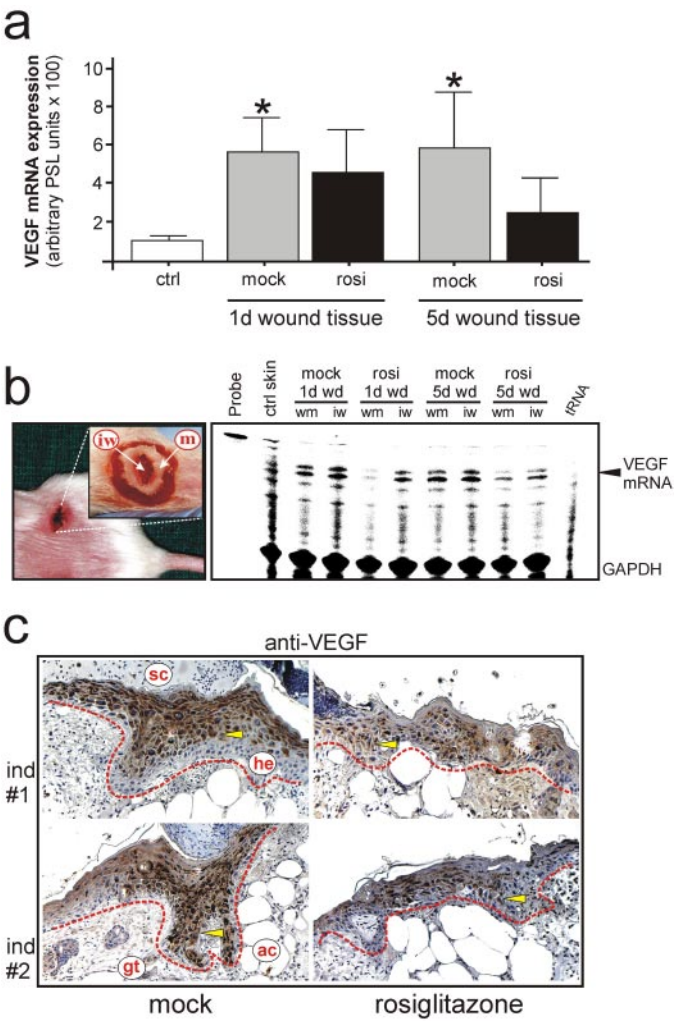

Fig. 10. Rosiglitazone impairs VEGF expression from keratinocytes in acute wounds of *ob/ob* mice. a, VEGF mRNA expression in total wound tissue of nontreated (mock) or rosiglitazone (rosi)-administered ob/ob mice was determined 1 day (1 d wound tissue) or 5 days (5 d wound tissue) upon injury by RNase protection assay. Expression levels of VEGF mRNA are expressed as arbitrary PhosphorImager PSL units. *, $P < 0.05$ compared with nonwounded control skin (ctrl) (ANOVA, Dunett's method). Bars indicate the mean ± S.D. from four wounds ($n = 4$) from three individual mice ($n = 3$). b, overview to show tissue sampling for inner wound (iw) and wound margin (wm) compartments (left). RNase protection analysis of VEGF mRNA levels in wm and iw tissue compartments isolated from mock (mock)- or rosiglitazone (rosi)-treated ob/ob mice 1 day (1 d wd) and 5 days (5 d wd) upon injury. Ctrl skin refers to back skin biopsies of nonwounded mice. A tRNA was used to control the specificity of the VEGF antisense RNA. A simultaneous hybridization of GAPDH within the same samples served to control an equal loading. Every experimental time point depicts isolated wm and iw compartments from two wounds each ($n = 2$) obtained from three individual mice ($n = 3$), which have been pooled before analysis. c, paraffin-fixed sections from mouse wounds (day 5 after wounding) were incubated with a polyclonal goat antiserum directed against murine VEGF. Immunopositive signals within the sections are indicated with arrows. Wound margin epithelia are indicated by a red line. ac, adipocytes; gt, granulation tissue; he, hyperproliferative epithelium; sc, scab.

aimed to functionally connect the actions of PPARγ agonists specifically to keratinocytes. To circumvent this problem, we performed immunohistochemistry of wound tissue to allow an analysis of p38 activation in wound keratinocytes. As shown in Fig. 12, wound margin keratinocytes of troglitazone-treated mice expressed a robust presence of activated p38. The presence of phosphorylated p38 seemed enhanced compared with mock-treated animals, because nearly all keratinocytes exhibited a nuclear presence of phosphorylated p38 upon troglitazone treatment. The observed reduction of wound margin epithelia upon rosiglitazone treatment (Figs. 10 and 12) was also paralleled by an activation of p38, because again nearly all keratinocytes of the reduced epithelia stained for the phosphorylated kinase. It is important to note here that our histology-based data were in accordance to our in vitro findings from cultured keratinocytes: both PPARγ agonists had been inducers of p38 activation, but only troglitazone was capable to mediate a PPARγ-independent induction of VEGF expression in the cells.

Here, we further analyzed wound granulation tissue and scab for activated p38. We did so to explain the different signals for activated p38 in immunoblots and histologies: rosiglitazone-treated *ob/ob* mice showed an overall reduction, and troglitazone-treated mice showed any change in p38 activation in wound lysates (Fig. 11) in the presence of a significant phospho-p38 staining in keratinocytes (Fig. 12, second panel). Lower levels of activated p38 in immunoblots of total wound tissue upon rosiglitazone treatment seemed to reflect an overall reduction of phosphorylated p38 in wound macrophages (Fig. 12, third panel). According to the immunoblot (Fig. 11), troglitazone did not reduce activated p38 in wound macrophages compared with mock-treated mice (Fig. 12, third panel). Polymorphonuclear neutrophils did not contribute to this regulation, because this cell type did not express activated p38 (Fig. 12, bottom). In summary, the action of both PPARγ agonists on wound macrophages might explain, at least partially, the observed status of p38 activation in total wound tissues of TZD-treated mice.

PPARγ Agonists Do Not Interfere with Cytokine- and Growth Factor-Induced VEGF Expression in Keratinocytes. Finally, we tested the potency of rosiglitazone and troglitazone to interfere with keratinocyte responses toward wound-derived mediators such as cytokines and EGF. This was important, because VEGF expression from wound keratinocytes in rosiglitazone (reduced VEGF expression)- and troglitazone (robust VEGF expression)-treated *ob/ob* mice might not only be a result of the observed PPARγ-independent effects but might also be based on a functional interaction with responses of wound keratinocytes toward wound-derived mediators. To this end, we stimulated keratinocytes with submaximal concentrations of cytokines and EGF to enable a modulation of induced VEGF expression by the drugs. We determined the EC_{50} value for cytokine (combination of TNFα, 0.25 ng/ml; IL-1β, 0.5 ng/ml; IFNγ, 0.1 ng/ml) and EGF (2 ng/ml) stimulation (Fig. 13, top). Next, we stimulated keratinocytes with the assessed EC_{50} value of cytokines and EGF in the presence of increasing amounts of rosiglitazone and troglitazone, respectively. We did not observe any changes in cytokine- and EGF-induced VEGF expression in the presence of the respective PPARγ agonist (Fig. 13, bottom).

Discussion

The family PPARs seems to be an attractive group of proteins with promising novel therapeutical applications. In particular, PPARγ-activating TZDs have been developed to improve type 2 diabetes mellitus-associated insulin resistance (Staels and Fruchart, 2005). It is interesting that PPARγ might serve an integrative function at the interface between metabolic regulation and tissue movements. This notion seems to be even more important, because it has become evident that metabolism and inflammation are functionally connected through mechanisms of innate immunity

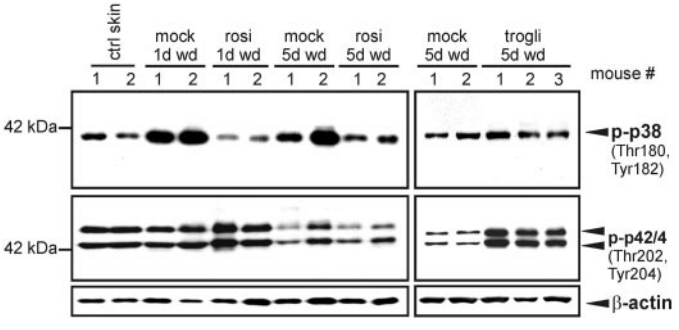

Fig. 11. Differential effects of PPARγ agonists in diabetes-impaired wound tissue: MAPK activation. Total wound tissue of nontreated (mock), or rosiglitazone- (rosi)-, and troglitazone (trogli)- administered *ob/ob* mice was analyzed for the presence of phosphorylated p38 MAPK (*p-p38, Thr180, Tyr182*) or phosphorylated p42/44 MAPK (*p-p42/44, Thr202, Tyr204*) by immunoblot. Mouse 1, 2, or 3 represent individual mice. Every experimental time point depicts two wounds ($n = 2$) obtained from an individual mouse, which have been pooled before analysis. β-Actin was used to control loading.

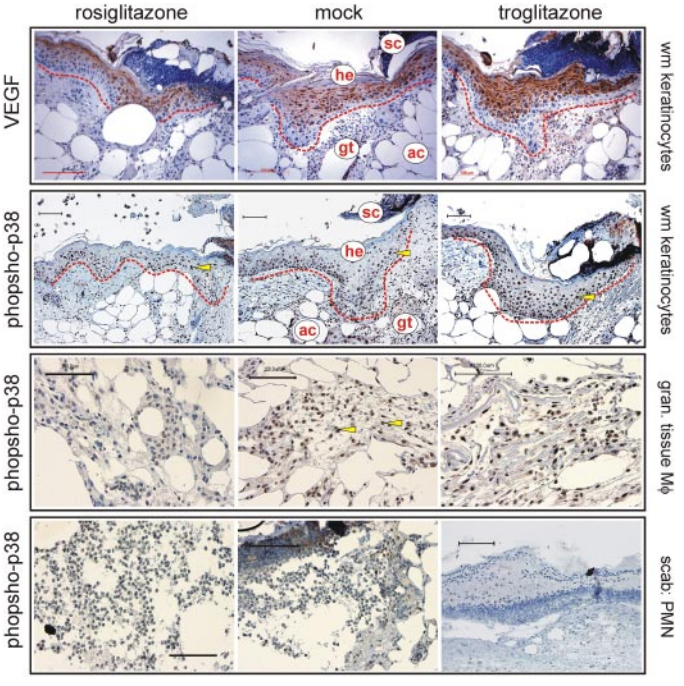

Fig. 12. Differential effects of PPARγ agonists in diabetes-impaired wound tissue: histology. Paraffin-fixed sections from mouse wounds (day 5 after wounding) were incubated with antisera directed against murine VEGF (top) or murine phosphorylated p38 MAPK (2–4). Immunopositive signals within the sections are indicated with arrows. Wound margin epithelia are indicated by a red line. ac, adipocytes; gt, granulation tissue; he, hyperproliferative epithelium; sc, scab. Scale bar, 100 μM.

(Hotamisligil, 2006). PPARγ participates in the control of fatty acid metabolism and the release of cytokines and adipokines from white adipose tissue (Rangwala and Lazar, 2004). In animal models of obesity, circulating levels of fatty acids (Delarue and Magnan, 2007), cytokines (Hotamisligil, 2006), and adipokines (Tilg and Moschen, 2006) are functionally connected to obesity-induced insulin resistance. At least in mice, skin tissue is known to differentially express all isoforms of PPAR (Michalik and Wahli, 2007) and represent an organ system susceptible of developing an obesity-mediated insulin resistance (Goren et al., 2006).

Diabetic conditions severely impair the healing process of cutaneous wounds in humans (Falanga, 2005) and in mice (Frank et al., 2000; Goren et al., 2003, 2006). In this context, it was tempting to argue for a possible function of therapeutically mediated PPAR activation to improve tissue movements during skin repair. In this study, we focused on the expression of VEGF for the following reasons: the expression of VEGF is markedly reduced in diabetes-impaired wounds (Frank et al., 1995), and keratinocytes represent the principal source of VEGF during skin repair (Brown et al., 1992) and express PPARα, -β/δ, and -γ isoforms (Michalik and Wahli, 2007).

In fact, both PPARα agonists, clofibrate and WY14643, completely failed to induce VEGF in HaCaT keratinocytes. Our observation is supported by findings from an epithelial colon carcinoma cell line, in which clofibrate and WY14643 were even potent suppressors of phorbolester-induced VEGF and Cox-2 expression. It is interesting that both substances inhibited DNA binding of activator protein-1 and thus transcriptional activation of VEGF and Cox-2 in a PPARα-dependent manner (Grau et al., 2006). By contrast, both the PPARβ/δ agonist L165,041 and the PPARγ agonists troglitazone and ciglitazone mediated a robust induction of VEGF mRNA and protein expression from cultured keratinocytes. This observation is in good accordance with recent findings in diverse cellular systems. Myofibroblasts exhibit a PPARγ-dependent biosynthesis of VEGF upon treatment with troglitazone and 15-deoxy-prostaglandin J2. In these cells, PPARγ-induced VEGF increase was functionally coupled to a decrease of nuclear factor-κB activity (Chintalgattu et al., 2007). In addition, bovine articular chondrocytes have been shown to up-regulate VEGF via oxidized low-density lipoprotein-mediated PPARγ activation (Kanata et al., 2006). However, the specific PPARγ inhibitor GW9662 suppressed oxidized low-density lipoprotein-induced VEGF expression in chondrocytes, providing evidence that PPARγ activation was, in contrast to keratinocytes, pivotal to VEGF expression. Nevertheless, the PPARγ agonist rosiglitazone failed to induce VEGF expression in keratinocytes, suggesting a different profile of pleiotropic actions for this member of the TZD family of drugs. It is interesting that it has been reported for several years that especially rosiglitazone provides antiangiogenic effects in endothelial and epithelial cells. In accordance to the failure of rosiglitazone to stimulate VEGF expression in keratinocytes (this study), it is noteworthy that this drug exerted antiangiogenic properties in particular by a marked reduction of VEGF biosynthesis during physiological processes such as endometrium-driven uterine angiogenesis (Peeters et al., 2005) and during pathophysiological processes such as angiogenesis in tumor growth and metastasis (Panigrahy et al., 2002).

There is growing evidence that activation of PPARβ/δ stimulates VEGF release in close functional connection to inhibition of apoptosis and stimulation of proliferation in human endothelial cells (Piqueras et al., 2007), colon carcinoma cells (Wang et al., 2006), and keratinocytes (Di-Poï et al., 2002). The potential of PPARβ/δ to trigger VEGF release in close functional connection to cell survival in a colon cancer cell line must be critically evaluated in the context of cancer development. By contrast, the ability of activated PPARβ/δ to drive VEGF expression (this study) and cell survival in ker-

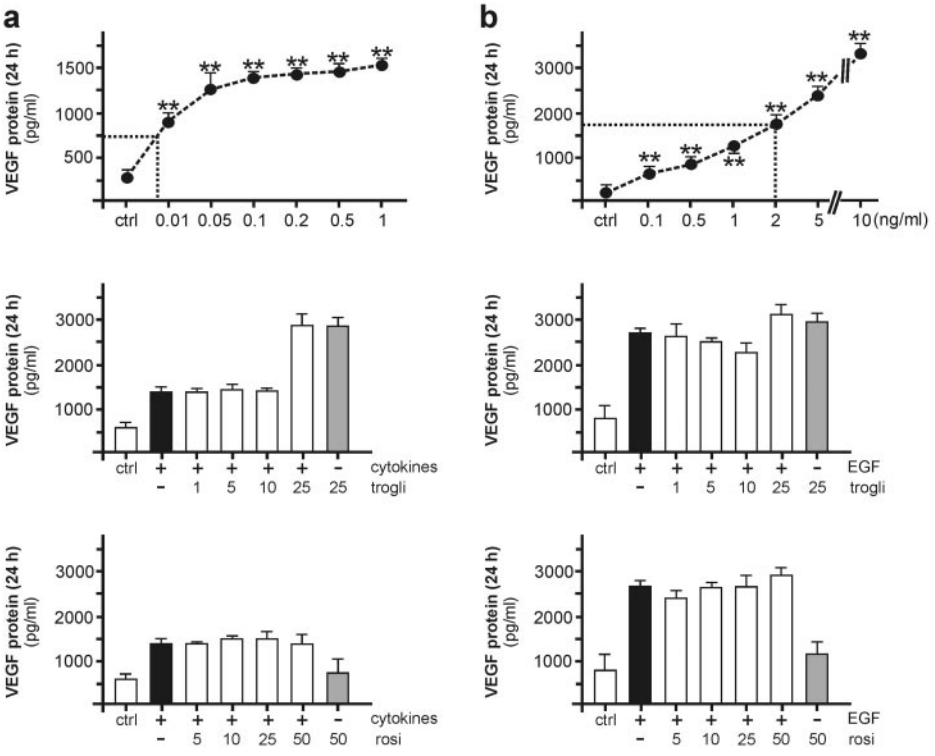

Fig. 13. PPARγ agonists do not interfere with cytokine- and EGF-induced VEGF expression in keratinocytes. a, quiescent human HaCaT keratinocytes were stimulated with increasing concentrations of cytokines (1 = TNFα, 25 ng/ml; IL-1β, 50 ng/ml; IFNγ, 10 ng/ml) (a) or EGF (0.1–10 ng/ml) (b) as indicated to determine the EC_{50} value. After 24 h, $VEGF_{165}$ protein release from the cells was assessed by ELISA analyses of the corresponding conditioned cell culture supernatants (top). Cells were subsequently stimulated with EC_{50} doses of cytokines (a, bottom) or EGF (b, bottom) in the presence or absence of troglitazone or rosiglitazone as indicated. **, $P < 0.01$ compared with nonstimulated control cells (ctrl). Bars indicate the mean ± S.D. from three independent cell culture experiments ($n = 3$).

atinocytes by activation of protein kinase B/Akt1 (Di-Poï et al., 2002) might be of functional importance in skin repair, where keratinocytes drive angiogenic processes via VEGF release (Brown et al., 1992; Frank et al., 1995) and cover the wound site from proliferative epithelia located at the margins of the wound (Singer and Clark, 1999).

In addition, it was reasonable and interesting to assess whether the observed unequal VEGF-stimulating capabilities of individual TZDs in cultured keratinocytes, even despite the observed independence of this process from binding to PPARγ, might also be transferred into diabetes-impaired wound conditions associated with disturbed angiogenic processes (Frank et al., 1995; Kämpfer et al., 2001; Eming and Krieg, 2006). Unfortunately, a functional role for PPARγ in skin repair still remains unresolved, especially because this receptor isoform was only hardly detectable in skin tissue upon injury (Michalik et al., 2001). Moreover, the role of PPARγ in the control of keratinocyte proliferation and differentiation still remains complex (Michalik and Wahli, 2007). The TZD ciglitazone mediated differentiation in human keratinocytes in vitro, as assessed by the induction of the typical keratinocyte differentiation markers involucrin and transglutaminase 1. A PPARγ-mediated process of differentiation could also be induced in murine epidermis, because ciglitazone induced the expression of keratinocyte differentiation markers loricrin and filaggrin in wild-type but not in PPARγ-null keratinocytes in mice (Mao-Qiang et al., 2004). In addition, PPARγ-independent effects seem to contribute to the TZD-mediated cellular decisions toward differentiation, because troglitazone caused a PPARγ-independent inhibition of keratinocyte proliferation by abrogation of cyclin D1 expression (He et al., 2004). In accordance to other reported PPARγ-independent mechanisms of TZDs in keratinocytes, we found that inhibition of p38 and p42/44 MAPK and not a functional ablation of PPARγ by siRNA abrogated TZD-stimulated VEGF expression in the cells. This observation confirms the findings of a most recent report on keratinocytes showing that troglitazone-induced Cox-2 expression did not involve PPARγ but p42/44 activation (He et al., 2006).

It is interesting that our experiments on TZD actions in acute wound healing in diabetic *ob/ob* mice basically support our major findings obtained from cultured keratinocytes: troglitazone and rosiglitazone both activated p38 MAPK in the cells, whereas the failure to induce VEGF expression was restricted to rosiglitazone only. This observation was quite interesting, because it again demonstrated potent differences in pleiotropic actions associated with drugs belonging to the same class of substances. In particular, those differences between troglitazone, which was withdrawn from the market in 2000 because of its drug-induced side effects, and rosiglitazone, which is still considered safe and of current therapeutic use, might contribute to the overall safety of individual members of the TZD family of drugs. In addition, our data from diabetes-impaired wound tissue in vivo suggested a rosiglitazone-mediated inhibition of wound keratinocyte proliferation, probably via activation of PPARγ (Mao-Qiang et al., 2004). Thus, it is reasonable to argue that the reduced VEGF expression from wound margin epithelia upon rosiglitazone treatment might be partially explained by decreased keratinocyte cell numbers. By contrast, troglitazone did not interfere with the size of wound margin epithelia, revealing an additional difference between both TZD drugs. It is remarkable that the functional connection between troglitazone and VEGF expression via activation of p38 and p42/44 MAPK in cultured keratinocytes seemed to be a key regulatory mechanism in VEGF biosynthesis and in wound keratinocytes in vivo, because we could observe a ubiquitous appearance of activated p38 MAPK in VEGF-expressing wound margin keratinocytes. In summary, our data from cell culture and wound healing experiments suggested p38 MAPK activation as a side effect of TZDs; however, only troglitazone, but not rosiglitazone, seemed to translate p38 MAPK activation into a PPARγ-independent induction of VEGF from keratinocytes.

Acknowledgments

We are grateful to Dr. Elke Müller for determination of VEGF protein levels from mouse wound tissue.

References

Boukamp P, Petrussevska RT, Breitkreutz D, Hornung J, Markham A, and Fusenig NE (1988) Normal keratinization in a spontaneously immortalized aneuploid human keratinocyte cell line. *J Cell Biol* **106:**761–771.

Brown LF, Yeo KT, Berse B, Yeo TK, Senger DR, Dvorak HF, and van de Water L (1992) Expression of vascular permeability factor (vascular endothelial growth factor) by epidermal keratinocytes during wound healing. *J Exp Med* **176:**1375–1379.

Chintalgattu V, Harris GS, Akula SM, and Katwa LC (2007) PPAR-gamma agonists induce the expression of VEGF and its receptors in cultured cardiac myofibroblasts. *Cardiovasc Res* **74:**140–150.

Chomczynski P and Sacchi N (1987) Single-step method of RNA isolation by acid guanidinium thiocyanate-phenol-chloroform extraction. *Anal Biochem* **162:**156–159.

Delarue J and Magnan C (2007) Free fatty acids and insulin resistance. *Curr Opin Clin Nutr Metab Care* **10:**142–148.

Di-Poï N, Tan NS, Michalik L, Wahli W, and Desvergne B (2002) Antiapoptotic role of PPARbeta in keratinocytes via transcriptional control of the Akt1 signaling pathway. *Mol Cell* **10:**721–733.

Eming SA and Krieg T (2006) Molecular mechanisms of VEGF-A action during tissue repair. *J Investig Dermatol Symp Proc* **11:**79–86.

Faglia E, Favales F, and Morabito A (2001) New ulceration, new major amputation, and survival rates in diabetic subjects hospitalized for foot ulceration from 1990 to 1993: a 6.5 year follow-up. *Diabetes Care* **24:**78–83.

Falanga V (2005) Wound healing and its impairment in the diabetic foot. *Lancet* **366:**1736–1743.

Frank S, Hübner G, Breier G, Longaker MT, Greenhalgh DG, and Werner S (1995) Regulation of vascular endothelial growth factor expression in cultured keratinocytes. Implications for normal and impaired wound healing. *J Biol Chem* **270:**12607–12613.

Frank S, Stallmeyer B, Kämpfer H, Kolb N, and Pfeilschifter J (1999) Nitric oxide triggers enhanced induction of vascular endothelial growth factor expression in cultured keratinocytes (HaCaT) and during cutaneous wound repair. *FASEB J* **13:**2002–2014.

Frank S, Stallmeyer B, Kämpfer H, Kolb N, and Pfeilschifter J (2000) Leptin enhances wound re-epithelialization and constitutes a direct function of leptin in skin repair. *J Clin Invest* **106:**501–509.

Franke TF, Yang SI, Chan TO, Datta K, Kazlauskas A, Morrison DK, Kaplan DR, and Tsichlis PN (1995) The protein kinase encoded by the Akt proto-oncogene is a target of the PDGF-activated phosphatidylinositol 3 kinase. *Cell* **81:**727–736.

Friedman JM (2003) A war on obesity, not the obese. *Science* **299:**856–858.

Gordon S (2003) Alternative activation of macrophages. *Nat Rev Immunol* **3:**23–35.

Goren I, Kämpfer H, Podda M, Pfeilschifter J, and Frank S (2003) Leptin and wound inflammation in diabetic ob/ob mice: differential regulation of neutrophil and macrophage influx and a potential role for the scab as a sink for inflammatory cells and mediators. *Diabetes* **52:**2821–2832.

Goren I, Müller E, Pfeilschifter J, and Frank S (2006) Severely impaired insulin signaling in chronic wounds of diabetic ob/ob mice. A potential role of tumor necrosis factor-α. *Am J Pathol* **168:**765–777.

Grau R, Punzón C, Fresno M, and Iñiguez MA (2006) Peroxisome-proliferator-activated receptor alpha agonists inhibit cyclo-oxygenase 2 and vascular endothelial growth factor transcriptional activation in human colorectal carcinoma cells via inhibition of activator protein-1. *Biochem J* **395:**81–88.

Green LC, Wagner DA, Glogowski J, Skipper PL, Wishnok JS, and Tannenbaum SR (1982) Analysis of nitrate, nitrite and [^{15}N]nitrate in biological fluids. *Anal Biochem* **126:**131–138.

He G, Sung YM, and Fischer SM (2006) Troglitazone induction of COX-2 expression is dependent on ERK activation in keratinocytes. *Prostaglandins Leukot Essent Fatty Acids* **74:**193–197.

He G, Thuillier P, and Fischer SM (2004) Troglitazone inhibits cyclin D1 expression and cell cycling independently of PPARgamma in normal mouse skin keratinocytes. *J Invest Dermatol* **123:**1110–1119.

Henry RR (1997) Thiazolidinediones. *Endocrinol Metab Clin North Am* **26:**553–573.

Hotamisligil GS (2006) Inflammation and metabolic disorders. *Nature* **444:**860–867.

Kämpfer H, Pfeilschifter J, and Frank S (2001) Expressional regulation of angiopoi-

etin-1 and -2 and the tie-1 and -2 receptor tyrosine kinases during cutaneous wound healing: a comparative study of normal and impaired repair. *Lab Invest* **81:**361–373.
Kanata S, Akagi M, Nishimura S, Hayakawa S, Yoshida K, Sawamura T, Munakata H, and Hamanishi C (2006) Oxidized LDL binding to LOX-1 upregulates VEGF expression in cultured bovine chondrocytes through activation of PPAR-gamma. *Biochem Biophys Res Commun* **348:**1003–10010.
Kliewer SA, Forman BM, Blumberg B, Ong ES, Borgmeyer U, Mangelsdorf DJ, Umesono K, and Evans RM (1994) Differential expression and activation of a family of murine peroxisome proliferator-activated receptors. *Proc Natl Acad Sci U S A* **91:**7355–7359.
Kliewer SA, Umesono K, Noonan DJ, Heyman RA, and Evans RM (1992) Convergence of 9-cis retinoic acid and peroxisome proliferator signalling pathways through heterodimer formation of their receptors. *Nature* **358:**771–774.
Kömüves LG, Hanley K, Lefebvre AM, Man MQ, Ng DC, Bikle DD, Williams ML, Elias PM, Auwerx J, and Feingold KR (2000) Stimulation of PPARalpha promotes epidermal keratinocyte differentiation in vivo. *J Invest Dermatol* **115:**353–360.
Lehmann JM, Moore LB, Smith-Oliver TA, Wilkison WO, Willson TM, and Kliewer SA (1995) An antidiabetic thiazolidinedione is a high affinity ligand for peroxisome proliferator-activated receptor γ (PPAR γ). *J Biol Chem* **270:**12953–12956.
Mao-Qiang M, Fowler AJ, Schmuth M, Lau P, Chang S, Brown BE, Moser AH, Michalik L, Desvergne B, Wahli W, et al. (2004) Peroxisome proliferator-activated receptor (PPAR)-gamma activation stimulates keratinocyte differentiation. *J Invest Dermatol* **123:**305–312.
Michalik L, Desvergne B, Tan NS, Basu-Modak S, Escher P, Rieusset J, Peters JM, Kaya G, Gonzalez FJ, Zakany J, et al. (2001) Impaired skin wound healing in peroxisome proliferator-activated receptor (PPAR)α and PPARβ mutant mice. *J Cell Biol* **154:**799–814.
Michalik L and Wahli W (2007) Peroxisome proliferator-activated receptors (PPARs) in skin health, repair and disease. *Biochim Biophys Acta* **1771:**991–998.
Mosmann T (1983) Rapid colorimetric assay for cellular growth and survival: Application to proliferation and cytotoxicity assays. *J Immunol Methods* **65:**55–63.
Panigrahy D, Singer S, Shen LQ, Butterfield CE, Freedman DA, Chen EJ, Moses MA, Kilroy S, Duensing S, Fletcher C, et al. (2002) PPARgamma ligands inhibit primary tumor growth and metastasis by inhibiting angiogenesis. *J Clin Invest* **110:**923–932.
Peeters LL, Vigne JL, Tee MK, Zhao D, Waite LL, and Taylor RN (2005) PPARgamma represses VEGF expression in human endometrial cells: implications for uterine angiogenesis. *Angiogenesis* **8:**373–379.
Piqueras L, Reynolds AR, Hodivala-Dilke KM, Alfranca A, Redondo JM, Hatae T, Tanabe T, Warner TD, and Bishop-Bailey D (2007) Activation of PPARbeta/delta induces endothelial cell proliferation and angiogenesis. *Arterioscler Thromb Vasc Biol* **27:**63–69.
Rangwala SM and Lazar MA (2004) Peroxisome proliferator-activated receptor γ in diabetes and metabolism. *Trends Pharmacol Sci* **25:**331–336.
Rivier M, Safonova I, Lebrun P, Griffiths CE, Ailhaud G, and Michel S (1998) Differential expression of peroxisome proliferator-activated receptor subtypes during the differentiation of human keratinocytes. *J Invest Dermatol* **111:**1116–1121.
Singer AJ and Clark RAF (1999) Cutaneous wound healing. *N Engl J Med* **341:**738–746.
Staels B and Fruchart JC (2005) Therapeutic roles of peroxisome proliferator-activated receptor agonists. *Diabetes* **54:**2460–2470.
Stallmeyer B, Kämpfer H, Kolb N, Pfeilschifter J, and Frank S (1999) The function of nitric oxide in wound repair: inhibition of inducible nitric oxide-synthase severely impairs wound reepithelialization. *J Invest Dermatol* **113:**1090–1098.
Stallmeyer B, Pfeilschifter J, and Frank S (2001) Systemically and topically supplemented leptin fails to reconstitute a normal angiogenic response during skin repair in diabetic ob/ob mice. *Diabetologia* **44:**471–479.
Tilg H and Moschen AR (2006) Adipocytokines: mediators linking adipose tissue, inflammation and immunity. *Nat Rev Immunol* **6:**772–783.
Wang D, Wang H, Guo Y, Ning W, Katkuri S, Wahli W, Desvergne B, Dey SK, and DuBois RN (2006) Crosstalk between peroxisome proliferator-activated receptor delta and VEGF stimulates cancer progression. *Proc Natl Acad Sci U S A* **103:**19069–19074.

Address correspondence to: Dr. Stefan Frank, Pharmazentrum Frankfurt/ZAFES, Institut für Allgemeine Pharmakologie und Toxikologie, Klinikum der JW Goethe-Universität Frankfurt/M., Theodor-Stern-Kai 7, D-60590 Frankfurt/M., Germany. E-mail: s.frank@em.uni-frankfurt.de